

**Calculation of hyperfine coupling constants**  
**An *ab initio* MRD-CI study for nitrogen to analyse**  
**the effects of basis sets and CI parameters**

by BERND ENGELS and SIGRID D. PEYERIMHOFF

Lehrstuhl für Theoretische Chemie, Universität Bonn,  
Wegelerstraße 12, D-5300 Bonn 1, F.R. Germany

and E. R. DAVIDSON

Indiana University, Department of Chemistry,  
Chemistry Building, Bloomington, Indiana 47405, U.S.A.

(Received 20 March 1987; accepted 22 April 1987)

The hyperfine coupling constant for the nitrogen atom is evaluated by large-scale MRD-CI calculations. A detailed analysis of the charge density at the nucleus and the spin polarization in the 1s and 2s shell as a function of various technical parameters is undertaken. Various (*s*, *p*) AO basis sets and the influence of correlation orbitals is investigated as well as selection threshold and other properties in CI calculations. The best value, obtained for the isotropic hyperfine coupling constant in an *s*, *p*, *d* basis, based on theoretical judgment of 'best' quantities, is 9.9 MHz compared to 10.4509 MHz.

### 1. Introduction

The interaction between the nuclear spin and the spin of an unpaired electron in atoms or molecules causes a splitting of energy levels; this interaction is referred to as hyperfine interaction. From the experimental side microwave and beam techniques, among others, have been employed to measure these effects, and it is possible to extract from the measured data information about the unpaired spin distribution in the system. The analysis is generally undertaken in terms of an isotropic and anisotropic contribution [1].

The isotropic hyperfine coupling constant  $a_{\text{iso}}$ , also called Fermi contact term, is defined for the nucleus *N* as

$$a_{\text{iso}}^{\text{N}} = (8\pi/3)(g_e/g_0)g_{\text{N}}\beta_{\text{N}}\langle\delta(r_{\text{N}})\rangle_{\text{spin}}. \quad (1)$$

The terms  $g_e$  and  $g_0$  are the *g* values for the free electron and the electron in the free radical respectively. The ratio is taken to be unity. The quantities  $g_{\text{N}}$  and  $\beta_{\text{N}}$  are the nuclear *g* factor and the value for the nuclear magneton respectively.

This isotropic hyperfine coupling contribution is a direct measure of the net unpaired spin density at the nucleus *N*. Only *s* atomic orbitals make contributions to it.

The anisotropic (or dipolar) hyperfine coupling constant is given by

$$A_{zz} = (g_e/g_0)g_{\text{N}}\beta_{\text{N}}\langle(3z^2 - r^2)/r^5\rangle_{\text{spin}} \quad (2)$$

and is a measure for the spatial distribution of the spin density. It is zero for *s* orbitals and averages to zero in *S* states.

The majority of theoretical *ab initio* calculations on spin properties in molecules [2] are limited to the use of the unrestricted Hartree–Fock (UHF) method, but it is known that this method overestimates the spin polarization contribution to the total spin density. A modification of this method, the projected UHF (PUHF) procedure attempts to remedy the spin contamination problem, and it has been shown in many cases [3] that an improvement is obtained at least judged by a better agreement with experimental data. On the other hand, Chipman [4] has noted that UHF generally reproduces trends in hydrocarbon radicals better. But neither method is able to give a uniform agreement with experiment better than about 60 per cent.

In the past few years calculations for spin properties employing extended AO basis set and natural orbital CI wavefunctions have been published [5, 6]. Generally good agreement with experiment for both  $a_{\text{iso}}$  and  $A_{zz}$  is found, but in some cases the difference is about 40–50 per cent in  $a_{\text{iso}}$  whereas  $A_{zz}$  is always in good agreement with the values deduced from measurements. The cause for the large discrepancy is still unclear.

It is thus the goal of the present work to calculate the hyperfine coupling constants (hfcc) for a simple system and to systematically study the influence of the various ingredients in the theoretical treatment. The  $^4S$  ground state of nitrogen with the electronic configuration  $1s^2 2s^2 2px 2py 2pz$  is such a test system. The anisotropic (dipolar) part is zero in this case and the Fermi contact term  $a_{\text{iso}}$  is different from zero because of the spin polarization in the  $1s$  and  $2s$  shells. The SCF value  $a_{\text{iso}}^{\text{SCF}}$  is also zero whereas the measured value is 10.4509 MHz [7]. Hence the  $^4S$  state of nitrogen is an excellent system to study in which way the description of spin polarization effects influences the value of  $a_{\text{iso}}$ . All calculations employ correlated wavefunctions.

## 2. Calculations

All calculations are undertaken with multi-reference single and double-excitation configuration interaction (MRD–CI) wavefunctions [8]. In this case a set of dominant (or reference) configurations is chosen from which all single and double excitations are generated; these configurations (or the symmetry-adapted functions SAF therefrom) build the MRD–CI space. For very large spaces only those SAFs are included in the wavefunction which contribute more than a given threshold  $T$  to the total energy, measured relative to the energy of the reference species, while the effect of the unselected species to the total energy is included in a perturbation-like manner. In most cases the selection threshold  $T$  was set to zero, i.e. all SAFs of the MRD–CI space are included in the treatment. Details of the reference species or threshold are given in the respective section. In addition to the MRD–CI energy the energy corresponding to the full CI has been estimated in the standard manner [9]  $E(\text{full CI est}) = E(\text{MRD–CI}) + (1 - \sum_{\text{ref}} c_0^2) \times [E(\text{MRD–CI}) - E(\text{Ref})]$  whereby the term ref refers to all reference configurations. All calculations are undertaken in the  $D_{2h}$  point group.

The ground state SCF orbitals are employed in the MRD–CI expansion, unless specified otherwise. In some cases the  $1s$  core has been kept doubly occupied, as is done in standard MRD–CI calculations for excited states or potential energy curves. Similarly, the  $2s$  shell has been kept doubly occupied in some instances in order to differentiate between the  $1s$  and  $2s$  shell contribution. These calculations will be

referred to as core (one doubly occupied shell) calculations. In the standard calculations all electrons are included in the MRD-CI procedure. All virtual SCF MOs are allowed variable occupation in the MRD-CI treatment undertaken. The Fermi contact term has been coded according to the integral evaluation given by Buenker and Chandra [10].

### 3. Influence of the atomic orbital $s$ and $p$ basis

The AO basis employed in the calculation influences the isotropic hyperfine coupling constant  $a_{\text{iso}}$  in two ways. First of all, because of the delta function in equation (1) only the density at the nucleus contributes to  $a_{\text{iso}}$ . Secondly, the basis set has to be able to describe the spin polarization of the  $1s$  shell as well as that of the  $2s$  shell, because both contributions to the spin polarization are expected to be similar in magnitude, but of opposite sign [11]. In order to obtain experience with respect to the size and the kind of basis sets which are appropriate for hfcc calculations, we employed basis sets of different quality from Duijneveldt [12], Huzinaga [13] and Ruedenberg [14]. A gaussian  $s$  function with a very large exponent, referred to as cusp function, is also added in some cases as indicated in table 1. All calculations were carried out with two reference configurations, namely the ground state configuration and a configuration which results from a  $2s \rightarrow 3s$  single excitation relative to the ground state. The ground state configuration is thereby dominant with  $c^2 = 0.9845$ , while the other configuration has a contribution of about  $c^2 = 0.003$ . The selection threshold was  $T = 0.0$ , i.e. the entire MRD-CI space was used in the secular equations.

It is seen (table 1) that for a given  $9s5p$  choice the Huzinaga basis yields lower energies than those of the two other authors. This changes upon expansion of the  $s$  and  $p$  set so that both, the Duijneveldt and Huzinaga  $10s6p$  basis are almost equivalent energetically, while the  $11s6p$  set of Duijneveldt is superior to the other employing the same number of functions. The Ruedenberg basis gives higher energies than the others at each level. The SCF energy of the Duijneveldt basis sets are practically constant beyond  $12s7p$ , and this pattern is also observed (although not quite as strong) in the CI values.

Table 1 and figure 1 show that the Fermi contact term  $a_{\text{iso}}$  depends drastically on the AO basis sets employed; the variation of  $a_{\text{iso}}$  becomes less, however, with basis sets larger than  $11s6p$ . The effect of cusp functions is almost zero. The differences between the basis sets of different authors show a parallel pattern as is observed in the energies, i.e. a closer agreement between the Huzinaga and Duijneveldt basis than with that given by Ruedenberg.

To examine the reason for the improvement of  $a_{\text{iso}}$  upon extension of the basis set, the two points mentioned earlier must be considered. The error of the basis set for calculating the density at the nucleus  $|\Psi(r=0)|^2$  can be estimated by comparing the Hartree-Fock total electron density at the nucleus  $\delta_0 = \langle \delta(r_N) \rangle_{\text{charge}}$  for a given basis set with large STO basis set results for the isolated atoms [15], denoted as the exact SCF value in the table. The calculated values with their errors are listed in table 2. The quality of the basis sets in calculating  $\delta_0$  behaves again similar as in calculating the total energy. Huzinaga and Duijneveldt basis sets produce nearly the same  $\delta_0$  while the Ruedenberg basis sets are of lower quality. In the larger basis sets of Duijneveldt, i.e.  $13s8p$ , the error amounts to less than 2 per cent. The effect of cusp functions is small.

Table 1. Summary of the calculated energies and isotropic hcc  $a_N$  employing different contracted gaussian basis sets.

Basis	Duijneveldt				Ruedenberg				Huzinaga			
	SCF†, §/h	MRD-CI/h	Full CI est./h	$a_{iso}/\text{MHz}^\ddagger$	SCF/h	MRD-CI/h	Full CI est./h	$a_{iso}/\text{MHz}$	SCF/h	MRD-CI/h	Full CI est./h	$a_{iso}/\text{MHz}$
9s5p	0.3918	0.4788	0.4800	4.05	0.3888	0.4754	0.4765	0.62	0.3953	0.4830	0.4842	3.61
10s6p	0.3990	0.4895	0.4908	5.15	0.3957	0.4854	0.4866	2.58	0.3989	0.4891	0.4903	5.32
11s6p	0.3999	0.4909	0.4922	7.33	0.3978	0.4882	0.4895	4.93	0.3992	0.4896	0.4909	7.86
12s7p	0.4006	0.4924	0.4937	7.64	0.3996	0.4913	0.4926	6.66				
13s7p	0.4007	0.4926	0.4939	7.82								
13s8p	0.4008	0.4929	0.4943	7.82								
13s8pS*	0.4008	0.4929	0.4942	7.84								
13s8pS**	0.4008	0.4929	0.4943	7.86								
14s8p					0.4004	0.4922	0.4936	7.34				

† The Hartree-Fock limit is  $-54.4009$  h. In all tables the energies are given in hartree units ( $E_h$  or short h), unless specified otherwise.

‡ The experimental value is  $a_{iso} = 10.4509$  MHz.

§ All energies are taken relative to  $-54.0$  hartree, i.e. the total energy is  $-54.3918$  h etc.

\* The exponent of the cusp function is  $192368.6215 a_0^{-2}$ .

\*\* The exponent of the cusp function is  $299046.8604 a_0^{-2}$ .

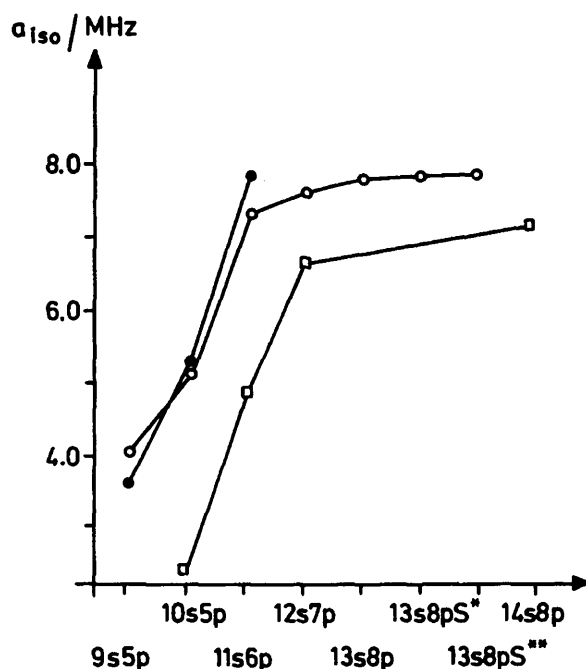


Figure 1. Dependence of the isotropic hfcc  $a_{iso}$  (in MHz) on different AO basis sets (2 reference configurations in the MRD-CI,  $T = 0$ ). ○, Duijneveldt; □, Ruedenberg; ●, Huzinaga. For details see table 1.

Next we have to study the ability of a basis set to describe the spin polarization. In order to distinguish between the 1s and 2s contributions the calculations are carried out such that a frozen 2s shell is maintained in investigating the 1s polarization while the 2s contribution is obtained in a calculation with a frozen 1s shell. Table 3 gives the results of such core calculations in the Duijneveldt basis set series. It is seen that both the 1s polarization and the 2s polarization increases (in absolute value) with the AO flexibility whereby a larger increase (about 3 times that found for 1s) is seen for the 2s polarization.

Table 2. Hartree-Fock total electron densities  $\langle \delta(r_N) \rangle$  at the nucleus.

Basis	Duijneveldt		Ruedenberg		Huzinaga	
	$\langle \delta(r_N) \rangle$	Error/per cent	$\langle \delta(r_N) \rangle$	Error/per cent	$\langle \delta(r_N) \rangle$	Error/per cent
9s5p	196.9	4.41	190.2	7.67	195.4	5.15
10s6p	198.8	3.50	194.6	5.53	199.0	3.40
11s6p	200.6	2.62	194.6	5.53	200.6	2.62
12s7p	201.9	1.99	198.2	3.79		
13s8p	203.0	1.45				
13s8pS*	203.6	1.17				
13s8pS**	204.1	0.92				

$\langle \delta(r_N) \rangle_{\text{exact}} = 206.0$  (near Hartree-Fock value).

\* The exponent of the cusp function is  $192368.6215 a_0^{-2}$ .

\*\* The exponent of the cusp function is  $299046.8604 a_0^{-2}$ .

Table 3. The 1s and 2s contribution to  $a_{\text{iso}}$  as a function of flexibility in the basis sets of Duijneveldt ( $T = 0.0$ ).

Contribution	9s5p	10s6p	11s6p	12s7p	13s8p	13s8pS*	13s8pS**
1s $a_{\text{iso}}$ /MHz	-52.81	-53.50	-53.97	-54.32	-54.62	-54.80	-54.93
2s $a_{\text{iso}}$ /MHz	53.02	54.73	57.31	57.98	58.52	58.71	58.85

The increase in polarization can be rationalized by looking at the behaviour of the orbital energies. Table 4 shows the effects of the basis set extension (Duijneveldt basis) on various AOs, characterized by their eigenvalues. The two double occupied orbitals remain essentially unchanged. The major contribution of the more diffuse functions included in the larger AO sets is found in the virtual orbitals; they possess low (positive) orbital energies, an effect which can be directly related to the more extended charge distribution in space. In this connection one must remember that actual Rydberg orbitals approaching the ionization limit converge to an orbital energy of zero. It is seen in table 4 that the 3s and 4s virtual orbitals exhibit only a minor change in orbital energy from basis 11s6p to 13s8pS\*\* while the higher-lying MOs are affected much more. Because of the lower energies of the virtual orbitals the possibility of making excitations to them is improved, which in turn leads to an increased spin polarization. The factor 3 between the increase of 1s and 2s polarization is reasonable since the energy gap between 1s and the virtual AOs is about an order of magnitude larger than between them and 2s.

A diagonalization of the one-electrons total spin density matrix (TSM) leads to eigenvalues and eigenvectors which give some insight into the mechanism for 1s and 2s polarization due to the virtual s orbitals. We call the new basis in which the total spin density matrix is diagonalized, a spin natural orbital (SNO) basis, in analogy to natural orbitals (NOs) which are obtained from diagonalization of the one electron (spatial) density matrix. The eigenvalues of the SNOs give a measure for the spin polarization of the AOs. They show equivalent trends as the core calculations discussed so far. It is found that in the TSM the off-diagonal elements are an order of magnitude larger than the diagonal elements. This implies a strong coupling of the AOs which combine to create the SNOs.

In table 5 the results of the diagonalization of the TSM is given. From the eigenvectors it is seen that in the 9s5p basis both the SNO1 and SNO2 are dominated by AO1 and AO4. The first is equivalent to the original 1s orbital while the second is a virtual s orbital with eigenvalue 8.9318 according to table 4. All other contributions are small. In the larger 13s8pS\*\* basis the contributions to SNO1 and

Table 4. Orbital energies (in hartree units) of the six lowest s orbitals ( $A_{1g}$  symmetry) in the Duijneveldt basis sets series.

Orbital	9s5p	10s6p	11s6p	12s7p	13s8p	13s8pS**
1s	-15.6254	-15.6282	-15.6287	-15.6290	-15.6291	-15.6291
2s	-0.9435	-0.9448	-0.9451	-0.9453	-0.9453	-0.9453
3s	0.9568	0.7055	0.4841	0.4334	0.3777	0.3777
4s	8.9318	4.4704	2.7938	2.4509	2.0563	2.0563
5s	44.4033	20.0204	12.6594	9.9350	7.4237	7.4237
6s	167.8720	76.2256	47.7572	33.8433	23.2307	23.2307

Table 5. (a) Diagonalization of total spin density matrix for the basis  $9s5p$  of Duijneveldt.

	Eigenvalue	Eigenvectors					
		AO1	AO2	AO3	AO4	AO5	AO6
SNO1	-0.00481	-0.70547	0.03821	-0.00812	0.70343	0.07726	0.0
SNO2	0.00482	0.70675	-0.03676	-0.01127	0.70220	0.07708	0.0
SNO3	-0.11382	0.03862	0.69715	0.71583	0.00880	0.00289	0.0
SNO4	0.11761	-0.03639	-0.71496	-0.69814	0.01008	0.00298	0.0

Table 5. (b) Diagonalization of total spin density matrix for the basis  $13s8pS^{**}$  of Duijneveldt.

	Eigenvalue	Eigenvectors					
		AO1	AO2	AO3	AO4	AO5	AO6
SNO1	-0.00598	-0.70810	0.02481	0.12127	-0.46078	-0.49115	-0.17070
SNO2	0.00606	0.70478	-0.02224	0.12749	-0.49056	-0.46620	-0.16733
SNO3	-0.14866	0.02442	0.69534	0.69120	0.19497	-0.01044	-0.00538
SNO4	0.15402	0.02274	0.71790	-0.67031	-0.18613	0.01072	0.00539

SNO2 are distributed more over the virtual orbitals. The contributions of AO4 and AO5 (with eigenvalues 2.06 and 7.4 according to table 4) are nearly identical and those of AO3 and AO6 are smaller but also of equal magnitude. This shows in yet another manner that excitation to virtual orbitals become more important in the more flexible (larger) basis, or in other words, that the virtual space is better represented and allows for a more adequate description of the spin polarization. This behaviour is in agreement with the rationalization on the basis of the orbital energies.

The same scheme is applicable to SNO3 and SNO4 which are dominated by AO2 and AO3, whereby the first is equivalent to the  $2s$  orbital and AO3 to the first virtual  $s$  orbital. If one goes from the  $9s5p$  to  $13s8pS^{**}$  set, the contributions of AO2 and AO3 remain nearly constant, whereas the mixing of all other AOs increases. Judged on the basis of orbital energies (table 4), AO2 is essentially the same in both basis sets whereas AO3 possesses an orbital energy of 0.9568 in the first and 0.3777 in the second basis; common to both AO3 is that they contain a marked contribution from the most diffuse AO in the basis. The increased mixing of other AOs is an indication that the larger basis is in a better position to describe the spin-polarization of a doubly-occupied orbital.

A comparison of the basis sets by various authors also shows differences in  $a_{iso}$ . The reason is probably the same as discussed above. The differences in the density at the nucleus  $\delta_0$  (table 2) are not large enough to explain the variances; the improvement in the description of the spin polarization is probably more important (tables 6, 7). The Duijneveldt  $11s6p$  basis set is more flexible in the valence region than the equivalent Ruedenberg basis set judged by considering the orbital energies (table 6). Its virtual AOs spread a larger range of electron distribution than the other bases, but the effect is clearly smaller than that between the Duijneveldt  $9s5p$  and  $13s8pS^{**}$  basis. From the core calculations (table 7) it seems as if the size and character of a basis set is more important for the  $2s$  polarization than for the  $1s$  polarization.

Table 6. Orbital energies (in hartree units) of the six lowest  $s$  orbitals ( $A_{1g}$  symmetry) using the  $11s6p$  basis sets.

Orbital	Huzinaga	Duijneveldt	Ruedenberg
1s	-15.6299	-15.6287	-15.6276
2s	-0.9453	-0.9451	-0.9447
3s	0.3409	0.4841	0.6702
4s	1.9264	2.7938	4.1376
5s	9.2156	12.6594	18.5148
6s	38.6173	47.7572	72.7736

Table 7. Core calculations for comparing the basis sets  $11s6p$  of different authors ( $T = 0.0$ ).

Contribution	Duijneveldt	Huzinaga	Ruedenberg
1s $a_{iso}$ /MHz	-53.97	-54.07	-52.91
2s $a_{iso}$ /MHz	57.31	58.11	54.01

In the entire discussion we have not mentioned  $p$  functions. Their influence on  $a_{iso}$  is clearly small, because  $|\Psi(r=0)|^2 = 0$  for such species. They have only a secondary effect via double excitations out of AO1 and AO2, i.e. for the description of electron correlation. Calculations with the Duijneveldt's  $13s7p$  and  $13s8p$  basis sets show no change, and hence no further analysis for  $p$  function influence has been made. These functions become important for calculations in molecules or in excited states of nitrogen.

#### 4. Influence of $d$ functions

In order to examine the influence of  $d$  polarization functions on  $a_{iso}$ , which are not contained in standard AO basis sets, but are known to be important for the description of electron correlation, the  $13s8p$  basis set of Duijneveldt is first contracted to  $8s4p$ . The contraction scheme (5, 2, 1, 1, 1, 1, 1) for the  $s$  functions and (4, 2, 1, 1) for the  $p$  functions gives the best energy result and was therefore used in the following calculations. In table 8 the results for various contractions are summarized. It is seen that the differences in  $a_{iso}$  are small.

To the contracted basis set first one  $d$  function is added and the exponent is optimized, always with respect to the total energy. For these calculations two different sets of reference configurations (table 9) are employed for the CI, namely a one main set which contains only the ground state configuration (referred to as 1

Table 8. Contraction of the ( $13s8p$ ) Duijneveldt basis to [ $8s4p$ ].

Contraction		SCF/h	MTD-CI/h	Full-CI est./h	$a_{iso}$ /MHz
$s$ -functions	$p$ -functions				
5 2 1 1 1 1 1 1	4 2 1 1	-54.40076	-54.47094	-54.47196	8.03
5 2 1 1 1 1 1 1	5 1 1 1	-54.40076	-64.46565	-54.46660	8.31
4 3 1 1 1 1 1 1	5 1 1 1	-54.40064	-54.46539	-54.46634	8.24
4 3 1 1 1 1 1 1	4 2 1 1	-54.40064	-54.47067	-54.47170	7.98

Table 9. The different sets of reference configurations employed in the calculations employing  $d$  functions. Their contribution to a final representative MRD-CI wavefunction is also given.

1M1R	$(1s)^2 (2s)^2$	$(2p_x)^1$	$(2p_y)^1$	$(2p_z)^1$	$c_1^2 = 0.9674$
4M1R	$(1s)^2 (2s)^2$	$(2p_x)^1$	$(2p_y)^1$	$(2p_z)^1$	$c_1^2 = 0.9674$
	$(1s)^2 (2s)^1 (3s)^1$	$(2p_x)^1$	$(2p_y)^1$	$(2p_z)^1$	$c_2^2 = 0.0027$
	$(1s)^2 (2s)^1 (d_{2x^2-y^2-z^2})^1$	$(2p_x)^1$	$(2p_y)^1$	$(2p_z)^1$	$c_3^2 = 0.0026$
	$(1s)^2 (2s)^1 (d_{x^2-y^2})^1$	$(2p_x)^1$	$(2p_y)^1$	$(2p_z)^1$	$c_4^2 = 0.0026$

main-1 root calculation: 1M1R) and a 4 reference configuration set. The latter is constructed by using the ground state and single excitations to the first virtual  $s$ -type orbital ( $3s$ ) and to the virtual  $d$ -type orbitals  $d_{2x^2-y^2-z^2}$  or  $d_{x^2-y^2}$  ( $s$ - and  $d$ -type orbitals belong to the same irreducible representation  $A_{1g}$ ). The corresponding calculations are referred to as 4M1R.

The results of the calculations are given in figure 2. It is seen that the value for

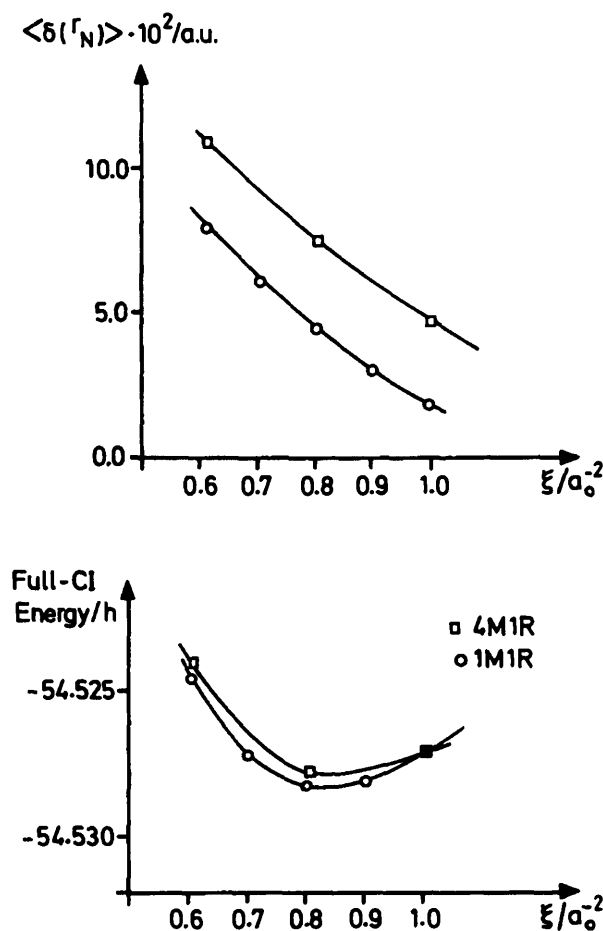


Figure 2. Calculated values for  $\langle \delta(r_N) \rangle$  and the total energy employing two different reference sets in the MRD-CI calculations as a function of the  $d$  function exponent  $\xi$ .

Table 10. Core calculations employing the [8s4p1d] Duijneveldt basis.

<i>d</i> -function exponent/ $a_0^{-2}$	$a_{\text{iso}}$ /MHz 1s contribution	$a_{\text{iso}}$ /MHz 2s contribution
0.6	-54.39	60.75
0.8	-54.42	57.31
1.0	-54.42	54.68

Table 11. Orbital energies (in hartree) of the lowest seven  $a_{1g}$  orbitals in the [8s4p1d] basis of Duijneveldt.

<i>d</i> exponent/ $a_0^{-2}$	1s	2s	3s	4s	$d_{2x^2-y^2-z^2}$	$d_{y^2-z^2}$	5s	6s
1.0	-15.629	-0.945	0.350	1.717	2.459	2.459	4.871	11.655
0.6	-15.629	-0.945	0.288	1.251	1.563	1.563	3.330	8.814

$\langle \delta(r_N) \rangle_{\text{spin}}$ , which is proportional to  $a_{\text{iso}}$  (see equation 1), decreases with increasing exponent of the *d*-function. The energy minimum is not accompanied by any special point in the  $\langle \delta(r_N) \rangle_{\text{spin}}$  graph.

Core calculations (table 10) show only a decrease of the 2s contributions within the limited exponent variation while the 1s contribution remain unchanged. Again a rationalization for this behaviour can be found in the spatial distribution of the *d* orbitals reflected in the orbital energies (table 11). Higher virtual orbitals than the 8s orbital make no contribution and therefore their energies are not of interest in the present context. The energy gap between the 2s and the virtual AOs is much smaller than between the 1s and the virtual species; furthermore there is much less overlap between the relatively contracted 1s charge distribution and that of the *d* function compared to the overlap between 2s and *d*. Both effects explain that the 1s contribution to  $a_{\text{iso}}$  is less affected by this *d* function variation than that of the 2s. The differences between the 1M1R calculation and the 4M1R calculation will be discussed later.

When the basis set is enlarged by further *d* polarization functions whose electron distribution covers approximately the same space (i.e. the original exponent  $\zeta$  is modified to give  $\zeta_1 = 2\zeta$  and  $\zeta_2 = 0.5\zeta$  according to standard procedure) the influence of the exponents becomes, as expected, smaller (table 12). The reason for this behaviour lies in the smaller dependence of the 2s contribution on the higher exponents. Similarly the 1s contribution remains unchanged.

Table 12. Variation of data employing two *d* functions with exponents  $\zeta_1$  and  $\zeta_2$  [8s4p2d] basis ( $E_{\text{SCF}} = -54.40076$  h, 1M1R calculation,  $T = 0.0$ ).

<i>d</i> exponents		Core calculations				
$\zeta_1/a_0^{-2}$	$\zeta_2/a_0^{-2}$	MRD-CI/h	est. full CI/h	$a_{\text{iso}}$ /MHz	1s $a_{\text{iso}}$ /MHz	2s $a_{\text{iso}}$ /MHz
1.9	0.4	-54.53404	-54.53895	6.05	-53.60	57.89
1.9	0.5	-54.53547	-54.54035	5.50	-53.62	57.36
1.9	0.6	-54.53495	-54.53964	4.65	-53.67	56.56
1.7	0.5	-54.53534	-54.54020	5.41		
2.1	0.5	-54.53526	-54.54014	5.67		

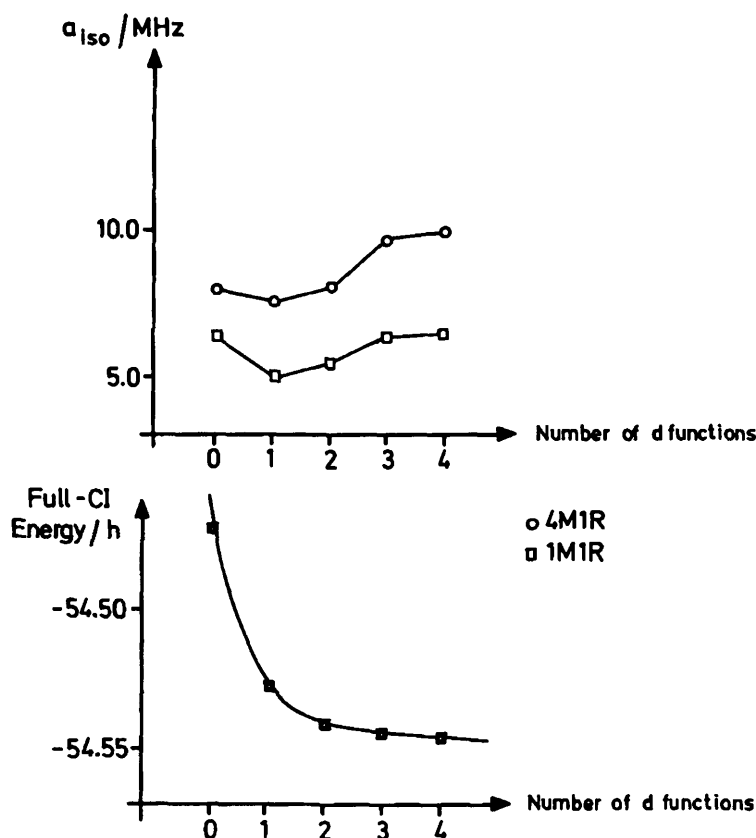


Figure 3. Behaviour of total energy and  $a_{150}$  upon addition of  $d$  functions.

Addition of more compact  $d$  functions to correlate the  $1s$  shell shows relatively little influence on the total energy (figure 3) but at first some surprising effect on  $a_{150}$ . The optimized  $d$  function exponents are listed in table 13 and it is seen that the standard rule of choosing exponents (multiplying the lower exponent always by a factor of four) as described by Flesh [16] is quite good. The value for  $a_{150}$  decreases first when going from zero to one  $d$  function (figure 3 and table 14) and returns to the original value in the 1M1R calculation only upon introduction of all four  $d$  species. If four reference configurations are employed instead, a definite improvement in  $a_{150}$  is seen upon introducing the more compact (No. 3, 4) species. An examination of the selection threshold will show later on that the increase from  $T = 0.0$  to  $T = 5 \times 10^{-10}$  hartree or  $T = 10^{-9}$  hartree, which was necessary in

Table 13. Optimized exponents of the  $d$  functions.

Number of $d$ functions	Exponents/ $a_0^{-2}$			
1	0.8			
2	0.5	1.9		
3	0.5	1.9	8.0	
4	0.5	1.9	8.0	39.0

Table 14. Summary of the calculated values by enlarging the basis set with  $d$  polarization functions.

Number of $d$ functions	1M1R calculation			4M1R calculation		
	MRD-CI/h	est. full CI/h	$a_{iso}$ /MHz	MRD-CI/h	est. full CI/h	$a_{iso}$ /MHz
0	-54.47053	-54.47189	6.48	-54.47094	-54.47196	8.03
1	-54.52414	-54.52817	4.98	-54.52533	-54.52780	7.61
2	-54.53547	-54.54035	5.50	-54.53696	-54.54029	8.10
3	-54.53851	-54.54350	6.34	-54.54003	-54.54346	9.74†
4	-54.54094	-54.54601	6.46	-54.54247	-54.54597	9.92‡

$E_{SCF} = -54.40076$  h, CI with selection threshold  $T = 0.0$ .

† Selection threshold  $T = 5 \times 10^{-10}$  h.

‡ Selection threshold  $T = 10^{-9}$  h.

order to keep the secular equation in the 3- $d$  and 4- $d$  calculations at manageable size, has no effect on the results. Note that the estimated full CI is about the same in both 1M1R and 4M1R treatments, as expected.

Core calculations (table 15) reveal that the total value of  $a_{iso}$  increases from the 1- $d$  to 4- $d$  calculation because the absolute value of the 1s contribution decreases faster than that of the 2s whereby the latter is almost constant when compact  $d$  functions are added. The definite decrease of both, 1s and 2s contribution to  $a_{iso}$  upon  $d$  function introduction can be rationalized. Introduction of  $d$  functions which are necessary to describe electron correlation change the total CI space so that excited configurations populating  $d$  orbitals are present. On the other hand,  $d$ -type orbitals make no contribution to  $a_{iso}$  because of their symmetry properties; hence the net effect is a reduction in  $s$ -type population, i.e. a reduction in  $a_{iso}$ . This effect can be seen directly in the eigenvalues of the spin natural orbitals SNOs listed in table 16. In the two lowest SNOs, which consist in the main of the 1s AOs the magnitude of the spin eigenvalue is reduced from 0.0061 to 0.0059 upon introducing the first  $d$  function. The situation in the two orbitals describing the 2s shell is similar, i.e. a reduction from 0.15 to 0.12 or from the 0.155 to 0.141. The parallel behaviour in 1s and 2s contribution obtained from core calculations and from this SNO analysis (carried out in the 4M1R treatment without any core) is also obvious from the table.

In table 17 the calculated correlation energies accounted for in the various calculations are summarized. It is seen that the first  $d$  function has by far the largest effect, in particular for the 2s shell, although the 1s shell also profits from it. The

Table 15. Core calculations for the basis set extension with  $d$  functions.

Number of $d$ functions	1s $a_{iso}$ /MHz	2s $a_{iso}$ /MHz	$a_{iso}$ /MHz	2s $a_{iso}$ /MHz
	1M1R	1M1R		4M1R
0	-54.91	58.75	3.84	59.37
1	-54.42	57.31	2.89	59.49
2	-53.62	57.36	3.74	59.53
3	-52.80	57.34	4.54	59.53
4	-52.80	57.40	4.60	59.59

Table 16. Eigenvalues of the most important SNOs in calculations employing zero to three  $d$  functions.

SNO1	1s	-0.00606	-0.00591	-0.00585	-0.00577
SNO2	1s	0.00611	0.00593	0.00588	0.00583
SNO3	2s/3s	-0.14986	-0.12333	-0.11962	-0.11985
SNO4	2s/3s	0.15527	0.14117	0.14104	0.14127
SNO5	$d_{2x^2-y^2-z^2}$		0.00346	0.00547	0.00548
SNO6	$d_{y^2-z^2}$		0.00346	0.00547	0.00548
1s contribution†		-54.91	-54.42	-53.62	-52.80
2s contribution†		58.75	57.31	57.36	57.34

†  $a_{iso}$  of the core calculations in MHz, from 1M1R treatment.

double- $\zeta$ -representation of the  $d$  function adds relatively little to the 2s correlation; the higher exponent obviously favours the 1s shell. Addition of the contracted 3d and 4d function affects only the correlation description in the 1s shell, as one would expect from the comparable spatial extension of the 3d and 4d orbitals and the 1s shell, listed in table 18. From this table it is also obvious that the 1d function matches the 2s optimally.

In summary then it is clear that the absolute magnitude of both the 1s and 2s contributions to  $a_{iso}$  decrease upon introduction of  $d$  orbitals because the  $d$  population does not contribute directly to  $a_{iso}$ . The first  $d$  species correlates primarily the 2s shell and therefore the decrease in the 2s shell contribution to  $a_{iso}$  is largest. Introduction of  $d$  functions with high exponents leave the 2s shell essentially unaffected and are correlation functions for the 1s shell; they are fairly contracted and show approximately the same radial distribution as the 1s shell (table 18). As a result the magnitude of the 1s contribution to  $a_{iso}$  keeps decreasing upon further inclusion of  $d$  correlation functions; the difference between the 2s and 1s contribution becomes larger and leads to the increase in the total value of  $a_{iso}$  from the 1-d to 4-d calculation (table 15). For a balanced treatment it is thus necessary to

Table 17. Calculated correlation energies (in eV)  $E(CI)-E(SCF)$  for various treatments employing from zero to four  $d$  functions.

Number of $d$ functions	All-electron calculations		Core calculations		
	1M1R	4M1R	1s	2s	
			1M1R	1M1R	4M1R
0-d	1.90	1.91	0.93	1.23	1.24
	1.93†	1.93†			
1-d	3.35	3.39	1.27(+36%)	2.67(+117%)	2.70(+118%)
	3.46	3.46			
2-d	3.66	3.71	1.42(+12%)	2.92(+9%)	2.96(+9%)
	3.79	3.79			
3-d	3.75	3.79	1.49(+5%)	2.93	2.97
	3.87	3.87			
4-d	3.81	3.86	1.55(+4%)	2.93	2.97
	3.94	3.94			

† Numbers in the second row always refer to the full CI estimate while otherwise the data from the MRD-CI calculations are taken.

Table 18. Expectation value of  $\langle r \rangle$  in  $a_0$  for the various AOs in the calculations employing from one to four  $d$  functions as a measure for their spatial extension.

AO	Calculations			
	1- $d$	2- $d$	3- $d$	4- $d$
1s	0.2283	0.2283	0.2283	0.2283
2s	1.3322	1.3321	1.3321	1.3322
3s	3.2026	3.0932	3.0935	3.1255
4s	1.4273	2.1194	2.1200	2.1851
1d	2.3493	1.8136	1.8161	1.8163
2d	—	1.0398	1.0459	1.0467
3d	—	—	0.5150	0.5202
4d	—	—	—	0.2266

account properly for both, the 1s and 2s shell correlation. The increase of the 2s contribution by changing from the 1M1R to 4M1R calculation lies in the fact that the new reference configurations with an open 2s shell (table 9) generate more 2s shell SAFs and hence more 2s shell contribution. The corresponding change upon introducing of open 1s shell reference configurations is much smaller.

### 5. Dependence on CI-selection threshold

In a standard calculation it is not economical to consider all single and double excitations from a set of reference configurations explicitly. In order to analyse the dependence of the calculated value of  $a_{\text{iso}}$  on the selection threshold  $T$  used in the MRD-CI program we performed calculations with the 8s4p2d basis described above. The total number of SAFs (symmetry adapted functions) for the 4M1R calculations is 17522 in this case, so that it is possible to perform in addition a calculation with the threshold  $T = 0.0$ .

To examine the influence of single excitations for hfcc calculations two computations were made for every threshold. One in which all single excitations are treated like all other configurations in the selection procedure and the other in which all single excitations relative to the ground state configuration are included automatically in the wavefunction. In figure 4(a)  $a_{\text{iso}}$  is given as a function of  $\log T$ . Figures 4(b)–(d) contain further information about the calculations.  $\sum \Delta E_i$  (unselected) means the sum of the energy lowerings produced by the SAFs which have not been selected. Figure 4(c) shows as a function of threshold  $T$  the size of the secular equation (SAFs) actually diagonalized. The third figure (figure 4(d)) gives the ground state eigenvalue of the largest secular equation, referred to as  $E(T)$ . Table 19 contains the results of different core calculations and in table 20 the results of the diagonalization of the total spin density matrices are given.

From figure 4(a) it is seen that  $a_{\text{iso}}$ , calculated with  $T = 10^{-5}$  h, i.e. by using about 5 per cent of the possible SAFs, is too high by about a factor of 3 if a selection among the single excitation configurations is undertaken. The value decreases drastically by lowering the selection threshold, and remains nearly constant from  $T = 10^{-8}$  h, when about 46 per cent of the possible SAFs are considered, to  $T = 0.0$ . If one takes all single excitations to the wavefunction, the calculated value of  $a_{\text{iso}}$  for  $T = 10^{-5}$  h is too low by about a factor of 0.5 and increases by

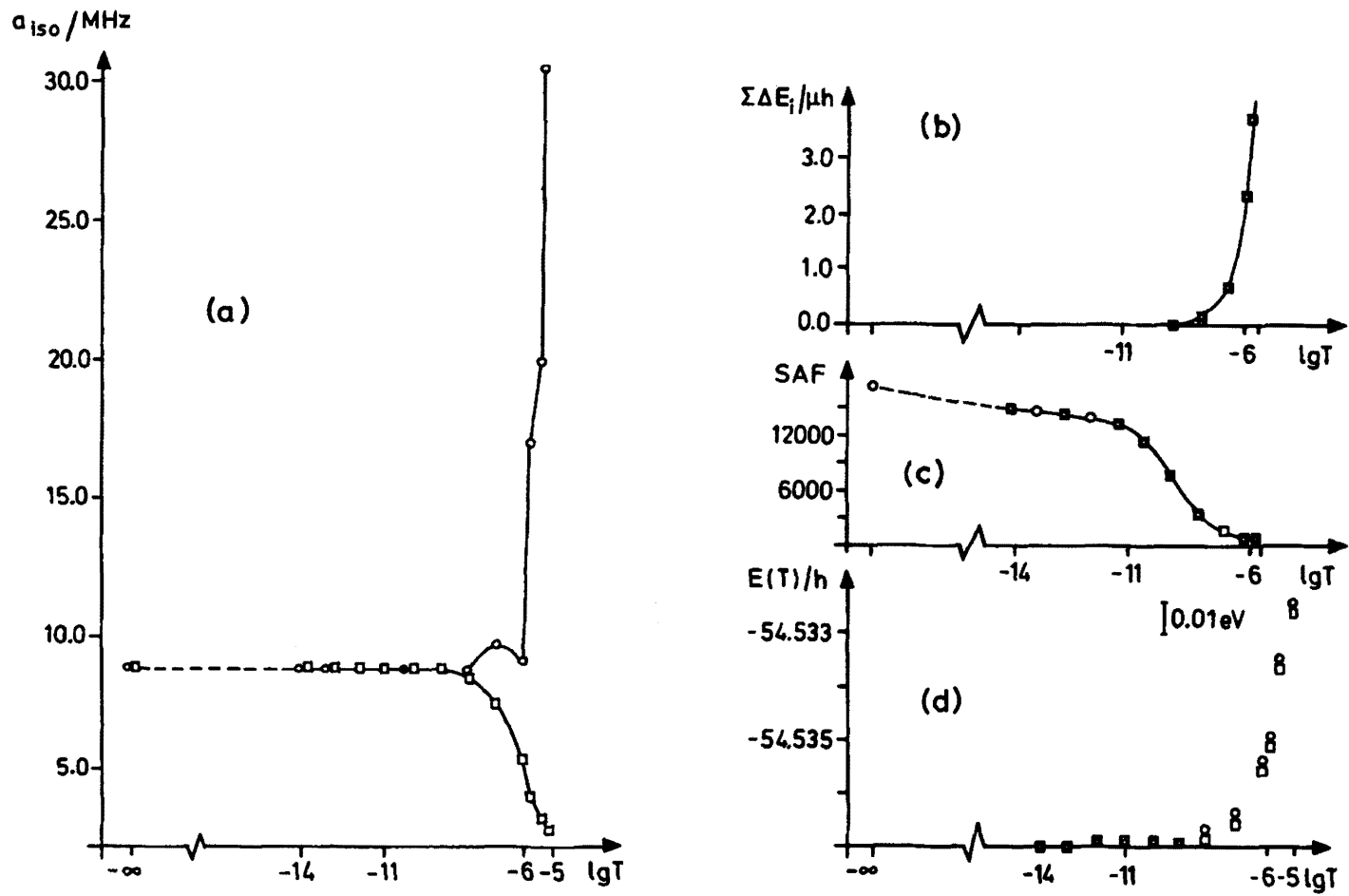


Figure 4. MRD-CI results as a function of the selection threshold  $T$ . 4M1R treatment,  $[8s4p2d]$  contracted basis. (a) The value of  $a_{iso}$  for the  $^4S$  state of the nitrogen atom in two treatments.  $\circ$ , standard selection procedure;  $\square$ , automatic inclusion of single excitations. (b) Sum of all energy contributions of the configurations not selected  $\Sigma \Delta E_i(T)$ , whereby  $\Delta E_i$  is the difference between the CI of the reference configurations and that in which  $\Psi_i$  is included. (c) Number of SAFs. (d) Eigenvalue  $E(T)$  of the largest secular equation actually solved;  $\circ$ , standard selection procedure;  $\square$ , automatic inclusion of single excitation.

Table 19. Core calculations at various selection thresholds. *E* = single excitations automatically included.

Contribution of	Selection threshold $T/10^{-6}$ h								
	10.0	10.0 <i>E</i>	6.0	6.0 <i>E</i>	1.0	1.0 <i>E</i>	0.1	0.1 <i>E</i>	0.0
1s $a_{\text{iso}}$ / MHz	-25.86	-53.77	-37.18	-53.68	-50.74	-53.68	-50.71	-53.64	-53.62
2s $a_{\text{iso}}$ / MHz	58.59	56.55	59.09	56.80	58.97	57.85	59.36	59.26	59.53

changing  $T$  to lower values. Again  $a_{\text{iso}}$  does not change if a selection threshold below  $10^{-8}$  h (corresponding to 8110 SAFs) is taken. The energy difference between the  $E(T)$  energy for  $T = 10^{-8}$  h and that for  $T = 0.0$  is only  $17 \text{ cm}^{-1}$ .

From table 19 it is obvious that the incorrect value of  $a_{\text{iso}}$  is obtained with standard selection of single excitations and a selection threshold of  $T = 10^{-5}$  h because the 1s contribution to  $a_{\text{iso}}$  is calculated much too small. The reason for this lies in the omission of excitations in higher MOs as it is shown by a comparison between the first and the third set of numbers in table 20. While the contribution of the AOs 7, 11, 12 to the SNO1/SNO2 is almost zero for  $T = 10^{-5}$  h they reach values about 0.25 when  $T$  is lowered to  $10^{-7}$  h. In comparison to the 1s contribution the 2s part is less affected; it increases slowly by 1 MHz (table 19). The contributions of the AO 7, 11, 12 to SNO3/SNO4 have about the same weight at the smaller threshold.

If one considers automatic selection of all single excitations the 2s contribution becomes the troublesome part (table 19, marked *E*), while the 1s contribution remains nearly unchanged by lowering the selection threshold  $T$ . The effects on  $a_{\text{iso}}$  are much smaller, however.

A comparison of the second and fourth set of numbers in table 20 does show some differences in the 2s contributions when changing from  $10^{-5}$  h to  $10^{-7}$  h. It seems that for  $T = 10^{-5}$  h the error in the wavefunctions from truncating less important double excitations and that which arises from omitting single excitations cancel each other approximately. By including all the single excitations relative to the ground state configuration the main error at  $T = 10^{-5}$  h occurs from omitting double excitations, and the calculated value of the 2s contribution is 56.55 MHz. By improving the wavefunction this error is also removed and for  $T = 10^{-7}$  h the 2s contribution reaches 59.26 MHz, which is close to the value of the calculation with  $T = 10^{-5}$  h, but without a general consideration of the single excitations. It is clear, however, that for smaller thresholds ( $T \leq 10^{-7}$  h) the 2s contribution is the same regardless of whether single excitations are included automatically or selected only via an energy criterium.

## 6. Summary and conclusion

In the present work we have analysed in which way the calculated hyperfine coupling depends on the ingredients of a standard *ab initio* calculation employing gaussian orbitals and correlated wavefunctions. As a test example the nitrogen atom in its  $^4S$  state has been chosen. In this case only the isotropic hyperfine coupling

Table 20. Diagonalization of the total spin density matrix obtained in the 4M1R calculation. Basis [8s4p2d].

Eigenvalue	AO1	AO2	AO3	AO6	AO7	AO10	AO11	AO12	AO13
Standard selection procedure, $T = 10^{-5}$ h									
SNO 1 -0.00468	-0.709	0.031	0.172	-0.469	-0.004	-0.497	0.0	0.0	0.0
SNO 2 0.00473	-0.702	-0.026	-0.174	-0.484	-0.008	0.489	0.0	0.0	0.0
SNO 3 -0.10951	0.029	0.672	0.696	0.251	-0.003	0.005	0.0	0.0	0.0
SNO 4 0.12980	-0.028	-0.739	0.634	-0.226	-0.001	-0.001	0.0	0.0	0.0
Inclusion of all single excitations, $T = 10^{-5}$ h									
SNO 1 -0.00596	-0.707	-0.030	-0.134	0.383	-0.268	0.406	0.294	0.109	-0.024
SNO 2 0.00595	-0.706	-0.027	-0.134	0.391	-0.268	0.399	0.294	0.110	-0.024
SNO 3 -0.11067	-0.029	0.673	-0.694	-0.254	-0.008	-0.003	0.011	0.002	0.0
SNO 4 0.13097	-0.028	-0.739	0.633	-0.229	0.007	0.001	0.010	0.003	0.0
Standard procedure, $T = 10^{-7}$ h									
SNO 1 -0.00585	-0.706	0.029	0.138	-0.395	0.263	-0.402	-0.286	-0.112	0.0
SNO 2 0.00582	-0.707	0.026	-0.138	0.404	-0.256	0.395	0.286	0.112	0.0
SNO 3 -0.11688	-0.028	0.674	0.698	0.242	-0.010	0.003	-0.010	0.003	0.0
SNO 4 0.13805	0.027	0.738	-0.637	-0.219	-0.008	-0.001	0.009	-0.003	0.0
Inclusion of all single excitations, $T = 10^{-7}$ h									
SNO 1 -0.00585	-0.706	0.029	0.138	-0.395	0.263	-0.402	-0.283	-0.112	0.012
SNO 2 0.00582	0.707	-0.026	0.138	-0.404	0.256	-0.395	-0.286	-0.112	0.012
SNO 3 -0.11688	-0.028	-0.674	-0.698	-0.242	0.010	-0.003	0.010	0.003	0.0
SNO 4 0.13805	-0.027	-0.738	0.637	0.219	-0.008	0.001	-0.009	-0.003	0.0

constant, which seems to be the quantity most difficult to represent in theoretical calculations, is different from zero.

The present investigations find that the quality in the description of the electron density at the nucleus  $\delta_0(r_N)$  parallels to a large extent that of a total energy description. It is therefore found that a quite flexible AO basis set is required. The (12s7p) gaussian set of Duijneveldt, for example gives an energy which is only  $3 \times 10^{-4}$  h above the Hartree–Fock limit and yields a value for  $\delta_0(r_N)$  of 201.9 compared to the Hartree–Fock limit of 206.0 [15]. This basis gives 7.64 MHz for  $a_{\text{iso}}$  when averaged over the spin functions, whereby the measured value is 10.45 MHz. Larger AO sets with *s* and *p* functions, in particular those including an *s* cusp function, lead only to minor improvements. Smaller basis sets such as (10s, 6p) or (9s, 5p) seem to be not sufficient for a reliable description of the hyperfine coupling constants. It is also found that the Duijneveldt and Huzinaga basis sets in the (11s6p) or smaller version are superior for energy and hfcc calculations compared to those of the same size given by Ruedenberg. A basis set contraction is also possible, just as in energy calculations, and a (13s8p) set contracted to [8s4p] has proven to be most profitable with respect to a loss in accuracy for energy and the hfcc value.

The description of spin polarization, which is the second important quantity in the evaluation of  $\langle \delta(\rho_N) \rangle_{\text{spin}}$ , depends on a very delicate balance of 1s and 2s shell polarization in nitrogen. It has been analysed by core calculations on one side (i.e. calculations with an alternative fixed 1s or 2s core), and by looking at the constitution of natural spin orbitals obtained by diagonalizing the total spin density matrix.

A more flexible AO basis allows for a better description of spin-polarization; this appears in form of various configurations in the CI expansion which possess single-occupied *s* shells. Their coefficients depend on the difference in energies between occupied and virtual orbitals and on the matching of their charge distribution. From this it is clear that the more flexible AO basis which covers a larger range in space gives a better representation of the spin polarization, in particular that of the 2s shell (but not negligible for the 1s shell). Introduction of *d* functions, which are necessary to account for electron correlation, decrease the magnitude of both, the 2s and 1s shell spin polarization. This is also to be expected since the extra configurations populating *d* species do not contribute to  $\langle \delta(r_N) \rangle_{\text{spin}}$  and as such reduce this value. The first *d* function generally correlates primarily the 2s shell and as a result  $a_{\text{iso}}$  decreases. Addition of more compact *d* functions to also account for an equivalent 1s shell correlation has the effect, that eventually the magnitude of 1s spin polarization decreases faster than that of the 2s shell with addition of contracted *d* species, which leads to an increase in the total value of  $a_{\text{iso}}$ .

The hfcc depends on details of the CI as long as only a small portion of the MRD–CI space is taken into account. The effect of single excitation configurations, which are relatively unimportant for energies, may seem to have a large effect on  $a_{\text{iso}}$  as long as a very selected subset of configurations is chosen. From the present calculations it looks as if the results do not change from a selection threshold of  $10^{-7}$  h to one of zero. On the other hand, this amounts to approximately one third of all SAFs generated in the MRD–CI space. Similar results have also been found in an entirely independent study [17] on the hfcc of  $\text{N}_4^+$  in which part of the work is also dedicated to the N atom, although not in as much detail as in the present work.

This finding could lead to a quite pessimistic view since the total MRD–CI space in realistic molecular calculations is in the order of  $10^6$  SAFs or more. On the other hand it is clear that the hfcc  $a_{\text{iso}}$  for nitrogen is very difficult to obtain, since it is

zero at the SCF or Hartree-Fock level and solely responsible to correlation effects. It is thus hoped that in molecular calculations some of the adverse effects in describing the hfcc cancel. But even if this is not the case, a route, similar to the energy calculation based on the present MRD-CI approach, could turn out to be feasible, namely a combined variational-perturbation or extrapolation-like treatment. This has been suggested earlier for one electron properties [18], whereby the density matrix at a given threshold obtained from the truncated MRD-CI wavefunction can be compared to that obtained from the reference set and the property can be extrapolated to zero threshold, i.e. the total space. Such procedure has not been necessary so far for standard properties such as electric dipole, transition dipole moments or various spin-orbit properties, but might well be necessary for hyperfine interactions which depend on electron correlation. Both ways, the influence of the molecular environment as well as a method to extrapolate from a representative portion of the configuration space to the total space will be studied for the hfcc in further work.

The authors want to thank D. Santry for constructing most of the computer code to evaluate the hyperfine properties on the basis of MRD-CI wavefunctions. The financial support given to this work by the Land Nordrhein-Westfalen is gratefully acknowledged. The services and computer time made available to the Computer Center of the University of Bonn have been essential to the present study.

#### References

- [1] WELTNER, W., JR., 1983, *Magnetic Atoms and Molecules* (Van Nostrand Reinhold).
- [2] AYSCOUGH, P. B., *Electron Spin Resonance*, Vol. 9 (Royal Society of Chemistry).
- [3] NAKASUJI, H., KATO, H., and YONEZAWA, T., 1969, *J. chem. Phys.*, **51**, 3175.
- [4] CHIPMAN, D. M., 1983, *J. chem. Phys.*, **78**, 4785.
- [5] FELLER, D., and DAVIDSON, E. R., 1984, *J. chem. Phys.*, **80**, 1006.
- [6] FELLER, D., and DAVIDSON, E. R., 1985, *Theor. chim. Acta*, **68**, 57.
- [7] ANDERSON, L. W., PIPKIN, F. M., and BAIRD, J. C., 1959, *Phys. Rev.*, **116**, 87. HOLLOWAY, W. W., LÜSCHER, E., and NOVICK, R., 1962, *Phys. Rev.*, **126**, 2109. HIRSCH, J. M., ZIMMERMANN III, G. H., LARSON, D. J., and RAMSEY, N. F., 1977, *Phys. Rev. A*, **16**, 484.
- [8] BUENKER, R. J., and PEYERIMHOFF, S. D., 1968, *Theor. chim. Acta (Berl.)*, **12**, 183. BUENKER, R. J., and PEYERIMHOFF, S. D., 1975, *Theor. chim. Acta (Berl.)*, **39**, 217.
- [9] LANGHOFF, S. R., and DAVIDSON, E. R., 1974, *Int. J. quantum Chem.*, **8**, 61. BUENKER, R. J., PEYERIMHOFF, S. D., and BRUNA, P. J., 1981, *Computational Theoretical Organic Chemistry*, edited by I. G. Csizmadia and R. Daudel (NATO ASI Series C, Vol. 67) (Reidel), p. 55.
- [10] CHANDRA, P., and BUENKER, R. J., 1983, *J. chem. Phys.*, **79**, 358.
- [11] POLING, S. M., DAVIDSON, E. R., and VINCOW, G., 1971, *J. chem. Phys.*, **54**, 3005.
- [12] VAN DUJNEVELDT, F. B., 1971, Tech. Report, IBM Research Laboratory, San Jose, California (RJ 945).
- [13] HUZINAGA, S., 1971, *Approximate Atomic Wavefunctions*, Vols. I and II (Department of Chemistry Report, University of Alberta, Edmonton).
- [14] SCHMIDT, M. W., and RUENDENBERG, K., 1979, *J. chem. Phys.*, **71**, 3951.
- [15] FRAGA, S., SAXENA, K. M. S., and LO, B. W. N., 1971, *Atom. Data*, **3**, 323.
- [16] FLESH, J., 1982, Dissertation, Kaiserslautern.
- [17] KNIGHT, L. B., JOHANSEN, C. D., EARL, E. A., FELLER, D., and DAVIDSON, E. R., *J. chem. Phys.* (submitted).
- [18] BUENKER, R. J., and PEYERIMHOFF, S. D., 1982, *New Horizons of Quantum Chemistry*, edited by P. O. Löwdin and B. Pullmann (Reidel), p. 183.